

Clean Absorption-Mode NMR Data Acquisition**

Yibing Wu, Arindam Ghosh, and Thomas Szyperski*

Multi-dimensional Fourier transform (FT) NMR spectroscopy is broadly used in chemistry^[1] and spectral resolution is pivotal for its performance. Phase-sensitive, pure absorption-mode signal detection^[1a,2] is required for achieving high spectral resolution as an absorptive signal at frequency Ω_0 rapidly decays proportional to $1/(\Omega_0 - \Omega)^2$, whereas a dispersive signal slowly decays proportional to $1/(\Omega_0 - \Omega)$. Therefore, a variety of approaches were developed to accomplish pure absorption-mode signal detection.^[1a,2] Moreover, by use of techniques such as spin-lock purge pulses,^[3] phase cycling,^[1a] pulsed magnetic-field gradients,^[4] or z-filters,^[5] radio-frequency (r.f.) pulse sequences for phase-sensitive detection are designed to avoid “mixed” phases, so that only phase errors remain which can then be removed by a zero- or first-order phase correction.

A limitation of the approaches^[1a,2] developed to date arises whenever the signals exhibit phase errors, which cannot be removed by a zero- or first-order correction, or when aliasing limits^[2a] the first-order phase corrections to 0° or 180° . Owing to experimental imperfections, such phase errors inevitably accumulate to some degree during the execution of radio-frequency (r.f.) pulse sequences^[1a,2] that results in superposition of the desired absorptive signals with dispersive signals of varying relative intensity which is not linearly correlated with Ω_0 . This situation not only exacerbates peak identification, but also reduces the signal-to-noise (S/N) ratio and shifts the peak maxima. In turn, this reduces the precision of chemical shift measurements and impedes spectral assignment based on matching of shifts.

Furthermore, phase-sensitive, pure absorption-mode detection of signals encoding linear combinations of chemical shifts relies on joint sampling of chemical shifts as in reduced-dimensionality (RD) NMR^[6] and its generalization, G-matrix Fourier transform (GFT) projection NMR.^[7] The GFT projection NMR is broadly employed, in particular also^[8] for projection-reconstruction (PR),^[9] high-resolution iterative frequency identification (HIFI),^[10] and automated projection (APSY) NMR.^[11] Importantly, the joint sampling of chemical shifts entangles phase errors from several shift

evolution periods. Thus, zero- and first-order phase corrections cannot be applied in the GFT dimension,^[7b] which further accentuates the need for approaches that are capable of eliminating (residual) dispersive components.

Herein we describe novel and generally applicable acquisition schemes for phase-sensitive detection of clean absorption-mode signals devoid of dispersive components. Those were established by generalizing mirrored time domain sampling (MS) to “phase-shifted MS” (PMS). MS was originally contemplated for absolute-value 2D resolved NMR spectroscopy^[12] and was later introduced for phase-sensitive measurement of spin-spin couplings in J-GFT NMR.^[7b] In general, the evolution of chemical shift α can be sampled as $c_{\pm n} = \cos(\pm \alpha t + n\pi/4 + \Phi)$, with “ \pm ” indicating forward (“+”) and backward (“−”) sampling, $n = 0, 1, 2$, or 3 yielding a phase shift by $n\pi/4$, and Φ representing the phase error giving rise to a dispersive component.

Forward sampling with $n = 0$ and 2 results in “States” quadrature detection,^[1a,2] which is herein denoted (c_{+0}, c_{+2}) -sampling and yields a signal $S(t) \propto \cos\Phi e^{i\alpha t} + \sin\Phi e^{i\pi/2} e^{i\alpha t}$. Corresponding backward (c_{-0}, c_{-2}) -sampling yields $S(t) \propto \cos\Phi e^{i\alpha t} - \sin\Phi e^{i\pi/2} e^{i\alpha t}$, so that addition of the two spectra (corresponding to “Dual States” $(c_{+0}, c_{+2}, c_{-0}, c_{-2})$ -sampling) cancels the dispersive components (Supporting Information, Section I.1). Thus, a clean absorption-mode signal $S(t) \propto \cos\Phi e^{i\alpha t}$ is detected (Figure 1).

Forward sampling and backward sampling with $n = 1$ results in (c_{+1}, c_{-1}) -PMS, which yields $S(t) \propto \cos\Phi e^{i\alpha t} - \sin\Phi e^{-i\alpha t}$ (Supporting Information, Section I.2). This implies that two absorptive signals are detected: the desired signal at frequency α with relative intensity $\cos\Phi$, and a quadrature image (“quad”) peak at frequency $-\alpha$ with intensity $\sin\Phi$. The (c_{+1}, c_{-1}) -PMS thus eliminates a dispersive component by transformation into an absorptive quad peak. Without phase correction, this results in clean absorption-mode signals (Figure 1). Corresponding (c_{+3}, c_{-3}) -PMS sampling yields $S(t) \propto \cos\Phi e^{i\alpha t} + \sin\Phi e^{-i\alpha t}$, so that the quad peak is of opposite sign when compared with (c_{+1}, c_{-1}) -PMS. Addition of the two spectra cancels the quad peak (Figure 1), and such combined $(c_{+1}, c_{-1}, c_{+3}, c_{-3})$ -sampling is named dual PMS (DPMS).

Forward sampling with $n = 0$ and backward sampling with $n = 2$ results in (c_{+0}, c_{-2}) -PMS yielding $S(t) \propto \cos\Phi e^{i\alpha t} - \sin\Phi e^{i\pi/2} e^{-i\alpha t}$ (Supporting Information, Section I.3), that is, the quad peak is dispersive. This feature allows the genuine and quad peaks to be distinguished, if required. In (c_{-0}, c_{+2}) -PMS, the quad peak is of opposite sign when compared with (c_{+0}, c_{-2}) -PMS, that is, $S(t) \propto \cos\Phi e^{i\alpha t} + \sin\Phi e^{i\pi/2} e^{-i\alpha t}$. Thus, $(c_{+0}, c_{-2}, c_{-0}, c_{+2})$ -DPMS likewise enables cancellation of the quad peak yielding solely clean absorption-mode signals.

PMS can be applied to an arbitrary number of indirect dimensions of a multi-dimensional experiment. For example, (c_{+1}, c_{-1}) -PMS of $K + 1$ chemical shifts $\alpha_0, \alpha_1, \dots, \alpha_K$ with phase

[*] Dr. Y. Wu, Dr. A. Ghosh, Prof. T. Szyperski
Department of Chemistry
State University of New York at Buffalo
Buffalo, New York 14260 (USA)
Fax: (+1) 716-645-6963
E-mail: szyperski@chem.buffalo.edu
Homepage: <http://www.chem.buffalo.edu/szyperski.php>

[**] This work was supported by NSF (MCB 0416899 and MCB 0817857) and NIH (P50 GM62413-01). We thank Drs. T. Acton and G. T. Montelione, Rutgers University, for providing the sample of protein Ca178.



Supporting information for this article is available on the WWW under <http://dx.doi.org/10.1002/anie.200804927>.

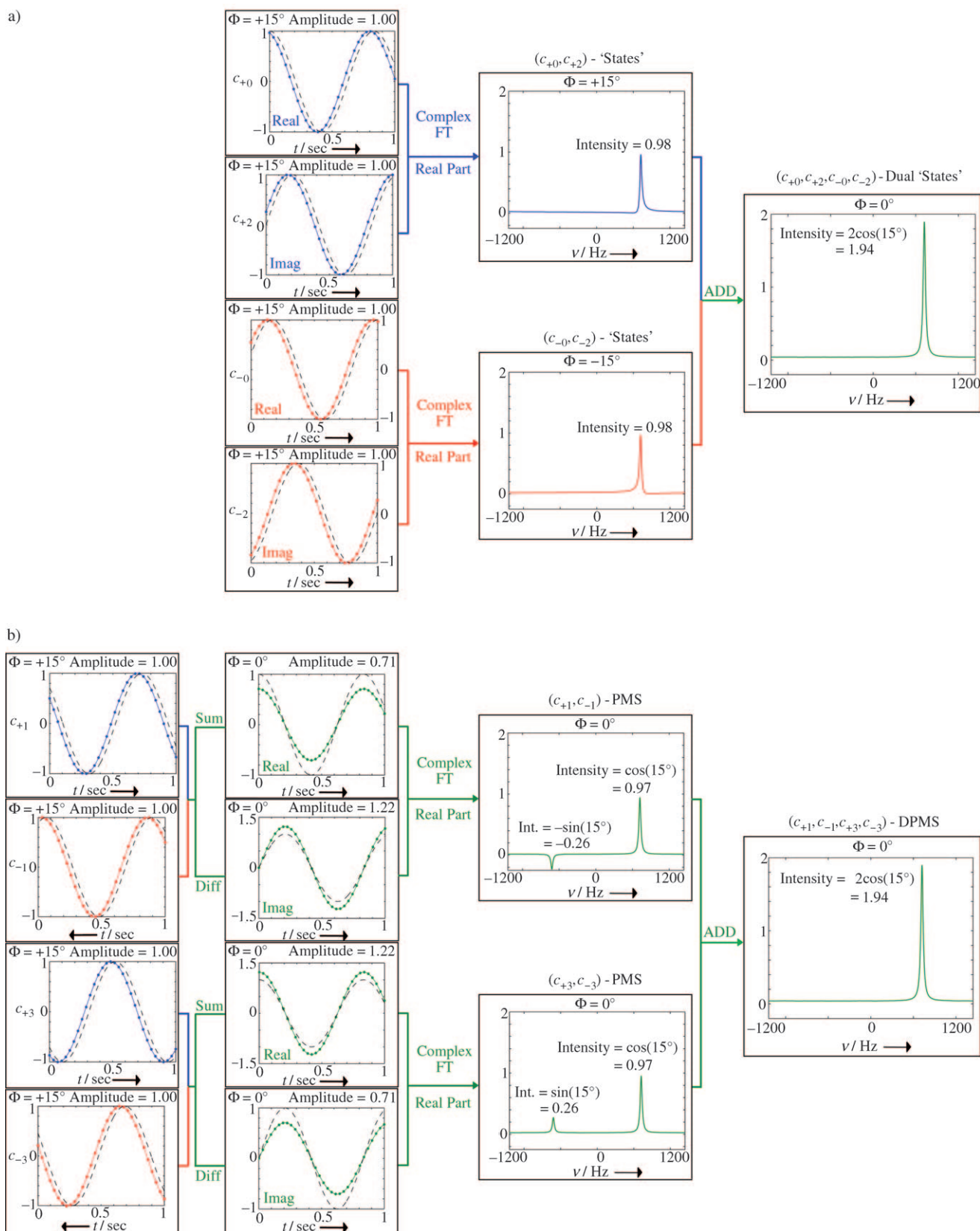


Figure 1. Clean absorption-mode NMR data acquisition a) dual “States” and b) $(c_{+1}, c_{-1}, c_{+3}, c_{-3})$ -dual phase shifted mirrored sampling (DPMS). The residual phase error Φ is assumed to be 15° . Forward time domain sampling and corresponding frequency domain spectra are shown in blue, backward time domain sampling and corresponding frequency domain spectra are shown in red, and linear combinations of time or frequency domain data are depicted in green. For comparison, the dashed gray lines represent time domain data of unit amplitude and $\Phi = 0$. In (a) the intensities of frequency domain peaks were calculated using Eq. S68 in the Supporting Information.

errors $\Phi_0, \Phi_1, \dots, \Phi_K$ (Supporting Information, Section I.4.1) yields a purely absorptive peak at $(\alpha_0, \alpha_1, \dots, \alpha_K)$ with relative intensity $\prod_{j=0}^K \cos \Phi_j$, whereas the quad peak intensities are proportional to $\cos \Phi_j$ for every $+\alpha_j$ and to $\sin \Phi_j$ for every $-\alpha_j$ in the peak coordinates. PMS can likewise be applied to an arbitrary subset of the chemical shift evolution periods jointly sampled in GFT NMR. For example, joint (c_{+1}, c_{-1}) -PMS of $K+1$ chemical shifts $\alpha_0, \alpha_1, \dots, \alpha_K$ (Supporting Information, Section I.4.2) yields a peak at the desired linear combination of chemical shifts with relative intensity of $\prod_{j=0}^K \cos \Phi_j$, whereas peaks located at different linear combinations of shifts exhibit intensities proportional to $\cos \Phi_j$ for all α_j for which the sign of the chemical shift in the linear combination does not change, and proportional to $\sin \Phi_j$ for all α_j for which the sign in the linear combination does change. Thus, PMS converts dispersive GFT NMR peak components into both quad and “cross-talk” peaks. For a given subspectrum, the latter peaks are located at linear combinations of chemical shifts, which are detected in the other subspectra.^[7] Furthermore, arbitrary combinations of time domain sampling schemes can be employed in multi-dimensional NMR, including GFT NMR (Supporting Information, Section I.4.3).

Clean absorption-mode data acquisition leads to a reduction of the signal maximum (and therefore the signal-to-noise ratio (S/N)) relative to a hypothetical absorptive signal by a factor of $\cos \Phi$ (see above). It is therefore advantageous to employ the commonly used repertoire^[1–5] of techniques to avoid phase corrections, so that only the residual dispersive components have to be removed. For routine applications, however, the reduction in S/N is then hardly significant: assuming that residual phase errors are $|\Phi| < 15^\circ$, a reduction of $< 3.4\%$ is obtained. Moreover, the superposition of a dispersive component on an absorptive peak in a conventionally acquired spectrum likewise reduces the signal maximum. As a result, the actual loss for $|\Phi| < 15^\circ$ is $< 1.7\%$ (Supporting Information, Section II, Figure S1).

(c_{+1}, c_{-1}) -PMS and (c_{+3}, c_{-3}) -PMS are unique as they yield clean absorption-mode spectra (Figure 1) with the same measurement time as is required for “States” acquisition. Whenever the quad peaks (and cross-talk peaks in GFT NMR), which exhibit a relative intensity proportional to $\sin \Phi$, emerge in otherwise empty spectral regions, they evidently do not interfere with spectral analysis and there is no need for their removal (when in doubt, (c_{+0}, c_{-2}) -PMS and (c_{-0}, c_{+2}) -PMS allows quad peaks to be identified as they are purely dispersive). Furthermore, sensitivity limited data acquisition^[6c] is often desirable (e.g., with an average S/N ca. 5). For $|\Phi| < 15^\circ$, $\sin \Phi < 0.26$ implies that quad and cross-talk peaks exhibit intensities circa 1.25 times the noise level, so that they are within the noise.

Suppression of axial peaks and residual solvent peaks is routinely accomplished using a two-step phase cycle.^[1a, 2a] In particular when studying molecules, which exhibit resonances close to those of the solvent line (e.g. $^1\text{H}^\alpha$ resonances of proteins dissolved in $^1\text{H}_2\text{O}$) such additional suppression of the solvent line is most often required. DPMS schemes can be readily concatenated with the two-step cycle (Supporting

Information, Section I.5), that is, DPMS spectra can be acquired with the same measurement as a conventional two-step phase-cycled NMR experiment. In solid state NMR,^[2b] artifact suppression relies primarily on phase cycling, and such concatenation of (multiple) DPMS and phase cycles enables clean absorption-mode spectra to be obtained without the investment of additional spectrometer time.

NMR spectra were acquired for $^{13}\text{C}, ^{15}\text{N}$ -labeled 8 kDa protein CaR178. First (c_{+1}, c_{-1}) -, (c_{+0}, c_{-2}) -PMS, and corresponding DPMS were implemented and tested for 2D [$^{13}\text{C}, ^1\text{H}$]-HSQC.^[2] The implementation of non-constant time^[2] “backward-sampling” required introduction of an additional 180° ^{13}C radio-frequency (r.f.) pulse (Supporting Information, Section III, Figure S2). As theory predicts, PMS and DPMS remove dispersive components and yield clean absorption-mode spectra without a phase correction (Supporting Information, Figure S3).

(c_{+1}, c_{-1}) -PMS and $(c_{+1}, c_{-1}, c_{+3}, c_{-3})$ -DPMS was then employed for simultaneous constant-time 2D [$^{13}\text{C}^{\text{aliphatic}} / ^{13}\text{C}^{\text{aromatic}}, ^1\text{H}$]-HSQC, in which aromatic signals are folded. As frequency labeling was accomplished in a constant-time manner,^[2] no r.f. pulses had to be added to the pulse scheme.^[2] The phase errors of the folded aromatic signals cannot be corrected after conventional data acquisition,^[1a] but are eliminated with PMS (Figure 2, Supporting Information, Figure S4).

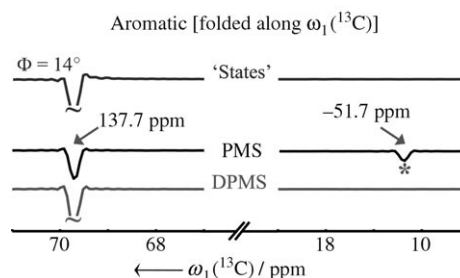


Figure 2. Cross sections along $\omega_1(^{13}\text{C})$ taken from 2D [$^{13}\text{C}^{\text{aliphatic}} / ^{13}\text{C}^{\text{aromatic}}, ^1\text{H}$]-HSQC acquired with States,^[1a] (c_{+1}, c_{-1}) -PMS, or $(c_{+1}, c_{-1}, c_{+3}, c_{-3})$ -DPMS. The “States” spectrum was phase-corrected such that aliphatic peaks are purely absorptive. This leads to a dispersive component in the aromatic peaks (top). The quad peak in the PMS spectra (middle) results from the dispersive component and is marked with (*). The quad peak is canceled in the clean absorption-mode DPMS spectrum (bottom). The actual chemical shifts (detected without folding) are indicated. (For data processing and contour plots, see Supporting Information Sections III and V, respectively.)

Multiple $(c_{+1}, c_{-1}, c_{+3}, c_{-3})$ -DPMS was exemplified for 3D HC(C)H total correlation spectroscopy (TOCSY).^[13] The ^{13}C - ^{13}C isotropic mixing introduces phase errors along $\omega_1(^{13}\text{C})$ that cannot be entirely removed by existing techniques. Moreover, in heteronuclear resolved NMR spectra comprising ^1H - ^1H planes with intense diagonal peaks (for example, HC(C)H TOCSY), even small phase errors impede identification of cross peaks close to the diagonal. As ^1H and ^{13}C frequency labeling was accomplished in a semi constant-time manner,^[2] no r.f. pulses had to be added to the pulse scheme.^[13] Comparison with the conventionally acquired

spectrum shows elimination of dispersive components in both indirect dimensions (Figure 3, Supporting Information, Figure S5).

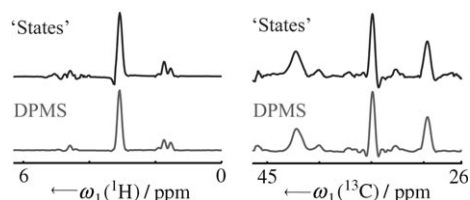


Figure 3. Cross sections taken along $\omega_1(^1\text{H})$ (left) and $\omega_2(^{13}\text{C})$ (right) from 3D HC(C)H TOCSY spectra recorded with either “States” quadrature^[1a] detection or DPMS in both indirect dimensions (for details of data processing, see Section IV of the Supporting information). DPMS yields a clean absorption-mode spectrum without applying a phase correction. Note that the dispersive components of the peak located approximately in the middle of the selected spectral range cannot be removed by a first-order phase correction. This would introduce dispersive components for other peaks located either up or downfield. (For data processing and contour plots, see Supporting Information Sections IV and V, respectively).

To exemplify multiple $(c_{+1}, c_{-1}, c_{+3}, c_{-3})$ -DPMS for GFT NMR,^[7] it was employed for $(4,3)\text{D } \underline{\text{C}}^{\alpha\beta}\underline{\text{C}}^{\alpha}(\text{CO})\text{NHN}^{[7b]}$ in both the $^{13}\text{C}^{\alpha\beta}$ and $^{13}\text{C}^{\alpha}$ shift evolution periods (the underlined letters denote jointly sampled chemical shifts). As frequency labeling was accomplished in a constant-time manner,^[2,7b] no r.f. pulses had to be added to the pulse scheme.^[7b] Comparison with standard GFT NMR shows elimination of dispersive components in the GFT-dimension (Figure 4, Supporting Information, Figure S6). Importantly, only PMS can eliminate entirely dispersive components in GFT-based projection NMR.^[7–11]

Dispersive components shift peak maxima (Supporting Information, Section II). For example, in routinely acquired $(4,3)\text{D } \underline{\text{C}}^{\alpha\beta}\underline{\text{C}}^{\alpha}(\text{CO})\text{NHN}^{[7b]}$ signals exhibit full widths at half height of $\Delta\nu_{\text{FWHH}} \approx 140$ Hz in the GFT dimension. As phase

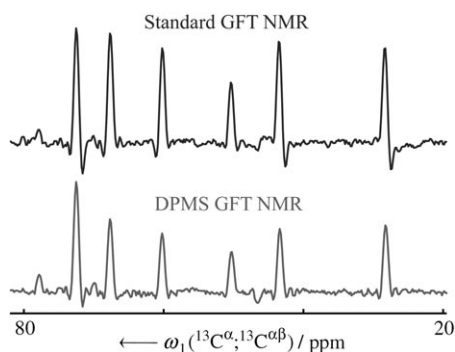


Figure 4. Cross sections along $\omega_1(^{13}\text{C}^{\alpha}, ^{13}\text{C}^{\alpha\beta})$ taken from the $\omega_2(^{15}\text{N})$ -projection of the $(4,3)\text{D } \underline{\text{C}}^{\alpha\beta}\underline{\text{C}}^{\alpha}(\text{CO})\text{NHN}^{[7b]}$ sub-spectrum comprising signals at $\Omega(^{13}\text{C}^{\alpha}) + \Omega(^{13}\text{C}^{\alpha\beta})$, recorded with standard GFT NMR data acquisition (top)^[4] or $(c_{+1}, c_{-1}, c_{+3}, c_{-3})$ -DPMS (bottom) for the jointly sampled chemical shift evolution periods. $(c_{+1}, c_{-1}, c_{+3}, c_{-3})$ -DPMS yields clean absorption mode GFT NMR sub-spectra (for details of data processing, see Section III of the Supporting Information). For data processing and contour plots, see Supporting Information Sections III and V, respectively.

errors up to about $\pm 15^\circ$ are observed, maxima are shifted by up to about ± 10 Hz (ca. ± 0.07 ppm at 600 MHz ^1H resonance frequency) and the precision of chemical shift measurements is reduced accordingly.

Clean absorption-mode NMR spectra are most amenable to automated^[14] peak “picking” and the resulting increased precision of shift measurements also increases the efficiency of automated resonance assignment of NMR spectra.^[15] This is because chemical shift matching tolerances can be reduced.^[16] Moreover, the enhanced spectral resolution promises to be of particular value for systems exhibiting very high chemical shift degeneracy such as (partially) unfolded or membrane proteins.

Taken together, clean absorption-mode NMR data acquisition also enables dispersive components arising from phase errors to be removed, which cannot be removed by a zero- or first-order phase correction. Thus, such data acquisition resolves a long-standing challenge of both conventional^[1a,2] and GFT-based projection NMR,^[7–11] and promises to have a broad impact on NMR data acquisition protocols for science and engineering.

Experimental Section

NMR spectra were acquired for $^{13}\text{C}, ^{15}\text{N}$ -labeled 8 kDa protein CaR178, a target of the Northeast Structural Genomics Consortium (<http://www.nesg.org>), on a Varian INOVA 600 spectrometer equipped with a cryogenic probe at 25 °C, and processed as described in the Supporting Information Section IV.

Received: October 9, 2008

Published online: January 12, 2009

Keywords: analytical methods · GFT projection NMR · NMR spectroscopy · phase-shifted mirrored sampling

- [1] a) R. R. Ernst, G. Bodenhausen, A. Wokaun, *Principles of Nuclear Magnetic Resonance in One and Two Dimensions*, Oxford University Press, Oxford, **1987**; b) N. E. Jacobsen, *NMR Spectroscopy Explained*, Wiley, New York, **2007**.
- [2] a) C. J. Cavanagh, W. J. Fairbrother, A. G. Palmer, N. J. Skelton, *Protein NMR Spectroscopy*, Academic Press, San Diego, **1996**; b) K. Schmidt-Rohr, H. W. Spiess, *Multidimensional Solid-State NMR and Polymers*, Academic Press, New York, **1994**.
- [3] B. A. Messerle, G. Wider, G. Otting, C. Weber, K. Wüthrich, *J. Magn. Reson.* **1989**, 85, 608–613.
- [4] J. Keeler, R. T. Clowes, A. L. Davis, E. D. Laue, *Methods Enzymol.* **1994**, 239, 145–207.
- [5] O. W. Sorensen, M. Rance, R. R. Ernst, *J. Magn. Reson.* **1984**, 56, 527–534.
- [6] a) T. Szyperski, G. Wider, J. H. Bushweller, K. Wüthrich, *J. Am. Chem. Soc.* **1993**, 115, 9307–9308; b) B. Brutscher, N. Morelle, F. Cordier, D. Marion, *J. Magn. Reson. Ser. B* **1995**, 109, 238–242; c) T. Szyperski, D. C. Yeh, D. K. Sukumaran, H. N. B. Moseley, G. T. Montelione, *Proc. Natl. Acad. Sci. USA* **2002**, 99, 8009–8014.
- [7] a) S. Kim, T. Szyperski, *J. Am. Chem. Soc.* **2003**, 125, 1385–1393; b) H. S. Atreya, T. Szyperski, *Proc. Natl. Acad. Sci. USA* **2004**, 101, 9642–9647; c) Y. L. Xia, G. Zhu, S. Veeraraghavan, X. L. Gao, *J. Biomol. NMR* **2004**, 29, 467–476; d) A. Eletsky, H. S. Atreya, G. Liu, T. Szyperski, *J. Am. Chem. Soc.* **2005**, 127, 14578–14579; e) S. Yang, H. S. Atreya, G. Liu, T. Szyperski, *J.*

- Am. Chem. Soc.* **2005**, *127*, 9085–9099; f) H. S. Atreya, T. Szyperski, *Methods Enzymol.* **2005**, *394*, 78–108; g) G. Liu, Y. Shen, H. S. Atreya, D. Parish, Y. Shao, D. K. Sukumaran, R. Xiao, A. Yee, A. Lemak, A. Bhattacharya, T. A. Acton, C. H. Arrowsmith, G. T. Montelione, T. Szyperski, *Proc. Natl. Acad. Sci. USA* **2005**, *102*, 10487–10492; h) H. S. Atreya, E. Garcia, Y. Shen, T. Szyperski, *J. Am. Chem. Soc.* **2007**, *129*, 680–692.
- [8] T. Szyperski, H. S. Atreya, *Magn. Reson. Chem.* **2006**, *44*, 51–60.
- [9] a) E. Kupce, R. Freeman, *J. Am. Chem. Soc.* **2004**, *126*, 6429–6440; b) B. E. Coggins, R. A. Venters, P. Zhou, *J. Am. Chem. Soc.* **2004**, *126*, 1000–1001.
- [10] H. R. Eghbalnia, A. Bahrami, M. Tonelli, K. Hallenga, J. L. Markley, *J. Am. Chem. Soc.* **2005**, *127*, 12528–12536.
- [11] S. Hiller, F. Fiorito, K. Wüthrich, G. Wider, *Proc. Natl. Acad. Sci. USA* **2005**, *102*, 10876–10881.
- [12] P. Bachmann, W. P. Aue, L. Müller, R. R. Ernst, *J. Magn. Reson.* **1977**, *28*, 29–39.
- [13] A. Bax, G. M. Clore, A. M. Gronenborn, *J. Magn. Reson.* **1990**, *88*, 425–431.
- [14] a) H. N. B. Moseley, N. Riaz, J. M. Aramini, T. Szyperski, G. T. Montelione, *J. Magn. Reson.* **2004**, *170*, 263–277; b) B. López-Méndez, P. Güntert, *J. Am. Chem. Soc.* **2006**, *128*, 13112–13122.
- [15] H. N. B. Moseley, D. Monleon, G. T. Montelione, *Methods Enzymol.* **2001**, *339*, 91–108.
- [16] For the program AutoAssign,^[15] a matching tolerance of $\delta = 0.3$ ppm is routinely used for $^{13}\text{C}^{\alpha/\beta}$ chemical shifts. As shifts of peak maxima are up to about $\delta = \pm 0.07$ ppm, elimination of dispersive components enables the tolerance to be reduced significantly.